Solubility of hydrogen in thin niobium films

J. Steiger, S. Blässer, and A. Weidinger
Hahn-Meitner-Institut Berlin GmbH, Bereich Schwerionenphysik, Glienicker Strasse 100, D-14109 Berlin, Germany
(Received 7 September 1993; revised manuscript received 3 November 1993)

The resonant nuclear reaction $^1H(^{15}N,\alpha\gamma)^{12}C$ was used to measure hydrogen concentrations in thin Nb films as a function of the external H_2 pressure (H solubility). Experiments were performed in the pressure range up to 1 mbar and temperatures between 166 and 200 °C, i.e., in the region around the critical temperature (177 °C) of the α-α' phase transition. We find that the hydrogen solubility in thin epitaxial films is considerably reduced compared to bulk data. The analysis of the data within mean-field theory for a lattice gas shows that the H-Nb interaction remains, within the experimental error, unchanged with respect to the bulk value but that the attractive H-H interaction energy is strongly reduced (0.1 eV in the film compared to 0.2 eV in the bulk). The difference is attributed to strain effects due to the clamping of the films to the substrate.

I. INTRODUCTION

Nb-H is one of the most studied and best-known systems in the field of hydrogen in metals and it is often considered as a model system for the study of the hydrogen interaction with metals.[1] It is known that Nb can dissolve large quantities of hydrogen (up to and exceeding [H]/[Nb]=2) and that a large variety of different phases can be formed.[1]

While these properties are well known for bulk materials, there is almost no information available about the behavior of hydrogen in thin epitaxial films. It can be expected that differences occur due to the clamping of the films to the substrate.[2–4]

It was shown that the hydrogen uptake in epitaxial Nb films leads, at low hydrogen concentrations, to a one-dimensional lattice expansion of the film in the direction normal to the surface, whereas the lateral dimensions remain unchanged.[3] At higher concentrations the lateral lattice constants change also but no precipitation of more concentrated phases was observed.[3] This finding was interpreted as evidence for the suppression of the α'- or β-phase formation in epitaxial films.

A disadvantage of these studies was that the hydrogen concentration in the films was not measured directly but was inferred from the lattice expansion and, therefore, was fairly uncertain. We report here studies of the hydrogen uptake in epitaxial Nb films with a direct measurement of the hydrogen concentration using a nuclear reaction. A further experimental improvement was that the concentration was measured while the sample was in contact with an external H_2 atmosphere, thus ensuring the thermodynamical equilibrium between the two systems.

II. EXPERIMENTAL DETAILS

A. Sample preparation

Thin Nb films were prepared by electron-beam evaporation in an ultrahigh vacuum system that had a base pressure in the 10^{-11}-mbar range. The substrate, a clean sapphire single crystal with a $(11\bar{2}0)$ orientation, was heated to a temperature of about 1000 °C during the film preparation. Under these conditions, Nb grows epitaxially with a (110) orientation.[5] On top of Nb, a thin layer of Pd was evaporated at room temperature in order to prevent Nb from oxidation and to enhance the H uptake rate during charging.[6] The thickness of the Nb layer was between 30–500 nm and that of the Pd layer on the order of 8 nm. The samples were characterized *in situ* by low-energy electron diffraction (LEED) to determine the surface structure and Auger-electron spectroscopy to check the purity of the surfaces.

B. Hydrogen-concentration measurement

Hydrogen depth profiles in the Nb layers were measured by the use of the nuclear reaction $^1H(^{15}N,\alpha\gamma)^{12}C$ which exhibits a sharp resonance at 6.385 MeV. The H depth profiles were obtained by recording the γ yield using a $6''\times6''$ NaI(Tl) scintillator as a function of the energy of the incoming ^{15}N ions.[7]

An essential part of the setup was a differential pumping system that allowed the performance of the experiments while the sample was in equilibrium with a H_2 atmosphere. For the solubility measurement, H_2 (99.999%), purified by a liquid-nitrogen cold trap, was let in by a precision valve. The H_2 pressure was measured by an absolute pressure gauge (Barocel 570, Datametrics). The sample was mounted on a target holder which could be heated up to 400 °C. The target cell was connected to the beam line via three apertures with 1, 2, and 3 mm diameters, respectively. Strong pumping units were installed between the apertures in order to reduce the pressure (maximum 1 mbar in the cell) to the beam-line vacuum.

No direct current measurement of the ^{15}N-ion beam was possible during H charging since discharges occurred when a suppression voltage was applied. We, therefore, used an α-Si:H film capped with a thin gold layer as a reference sample to record the beam intensity. Before

and after each energy change of the beam, the γ yield of this sample was measured and used to normalize the yield of the Nb sample. The absolute value of the H concentration was obtained by comparing the count rate with that of a Ta foil of known H content. A detailed description of the whole setup will be published elsewhere.[8]

III. SAMPLE CHARACTERIZATION

After removal from the UHV system, the samples were characterized by Rutherford backscattering spectroscopy (RBS) and x-ray diffraction (XRD). RBS with 2.4-MeV α particles was used to obtain the layer thicknesses and to test the homogeneity of the layers. We found no indications of an intermixing of Pd and Nb.

The XRD measurements were performed in standard Bragg-Brentano geometry ($\Theta-2\Theta$) using Cu $K\alpha_1$ radiation. In accordance with *in situ* LEED investigations, only reflections from sapphire ($11\bar{2}0$) and Nb (110) planes were found (Fig. 1) as expected from the known growth relationships of this system.[9] In most cases the out-of-plane coherence length of the Nb layers derived from the width of the (110) reflection agreed well with the total thickness of the Nb layers indicating that the films were of high quality. Rocking curves of the (110) line showed typically a width of 0.03° which has to be compared with values in the order of 0.07° for Nb-bulk single crystals.

Figure 2 shows a magnified view of the Nb (110) reflection. The "satellite" peaks seen in Fig. 2 result from the finite number of scattering planes. The distance of these finite thickness fringes is very sensitive to the number of coherent planes. A simulation of the diffraction pattern (solid line in Fig. 2) requires 340 planes, which together with the lattice constant of $a=0.33$ nm, yield a total thickness of 79 nm in good agreement with the thickness of 75 nm determined by RBS.

Remarkable in Fig. 2 is the asymmetry of the experimental fringes. This behavior is due to nonuniform lattice strains over the film thickness. A possible explanation is that the out-of-plane layer spacing is, due to the epitaxial growth, slightly larger for the near substrate layers than for the major part of the film. A study of thin

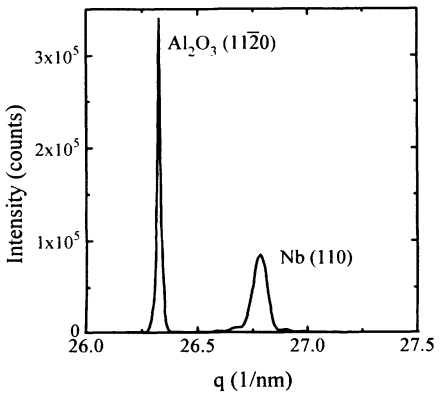

FIG. 1. Section of the x-ray diffraction diagram for a 79-nm-thick Nb layer on sapphire. Momentum transfer q is along the film normal. The whole diffractogram contains only reflections from the sapphire ($11\bar{2}0$) and the Nb (110) planes.

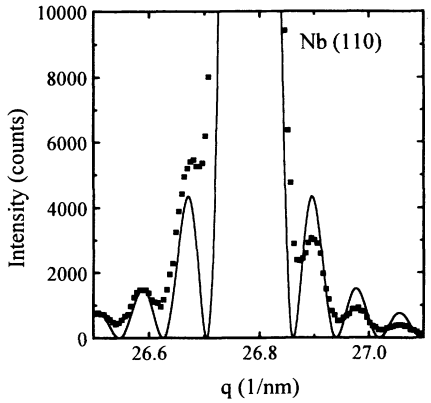

FIG. 2. Enlarged view of the Nb (110) reflection from Fig. 1. The solid line is the calculated line shape for a 79-nm-thick Nb film. The "satellite" peaks arise from the finite thickness of the film. The asymmetry in the intensities of the satellite peaks is due to strain present in the sample.

Ta layers on Al_2O_3 suggests that the in-plane lattice constants are expanded near the substrate.[10] From that, one might expect that then the out-of-plane lattice parameter would contract. Because of the similarity of Nb and Ta one would expect a similar behavior for Nb films. The present finding is not in accordance with this but the experiments are not completely comparable.

Another possibility is that the inhomogeneous hydrogen distribution in the as-deposited film (see Fig. 3), in particular the accumulation of hydrogen in the near-surface region, is responsible for the inhomogeneous strain. Such an explanation could also resolve the inconsistency mentioned above with the result of Ref. 10, since a hydrogen contamination would allow an expansion of the in-plane as well as the out-of-plane lattice parameters.

IV. SOLUBILITY MEASUREMENTS

Figure 3 shows the hydrogen-depth profiles of a 143-nm-thick Nb film at 200 °C before and after applying the

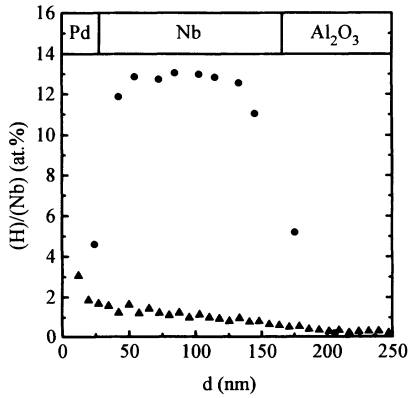

FIG. 3. H concentration in a Nb sample capped with Pd. The triangles show the uncharged case while the solid circles represent the concentration in equilibrium with a H_2 atmosphere at a pressure of 0.124 mbar. It can be seen that even the uncharged sample contains a H concentration of about 1 at. %.

H_2 atmosphere. The data points from the surface peak are beyond scale. In all cases we found a small but nonzero H concentration (<1 at. %) present in the Nb layers without charging. This initial H concentration is probably due to hydrogen bound to imperfections, like grain boundaries, and does not represent the equilibrium concentration corresponding to the partial pressure in the target chamber, although this concentration would not be much lower.

Increasing the H_2 pressure to 0.124 mbar leads to a rapid absorption of H within the Nb layer. The concentration increases to 13 at. % (plateau value) as seen in Fig. 3. Almost no H is dissolved in the Pd layer on top of Nb as can be deduced from the steep decrease of the concentration towards the surface. It should be noted that the thickness of the Nb layer derived from the ^{15}N energy loss (130 nm) is in fairly good agreement with the RBS value (143 nm) while it is off for the top-layer Pd (37 nm). However, the top layer has also a contribution from carbon deposition during the ion bombardment and this effect can explain the difference.

The measurements were performed with increasing and decreasing ion energy and lasted altogether several hours during which the H_2 atmosphere was present. The fact that no change in the γ yield was found between these runs (see Fig. 3) indicates that the equilibrium concentration had been reached. Similar measurements were performed on other samples that had different thicknesses and also the temperature was varied. The concentrations which are shown in the solubility curves were calculated from the plateau γ yield Y using the following relation:

$$\frac{[H]}{[Nb]} = k \left[\frac{dE}{dx} \right]_{Nb}^{-1} Y , \quad (1)$$

where $(dE/dx)_{Nb}$ is the specific energy loss of ^{15}N in Nb and k is a normalization constant which was determined by a calibration run with a Ta foil of known hydrogen concentration. Stopping powers were calculated with the program PRAL.[11,12]

The hydrogen solubility in Nb films with thicknesses between 70 and 560 nm is shown in Fig. 4. The temperature in this experiment was 200 °C which is slightly above the critical temperature for the α-α' phase transition. Also shown in Fig. 4 are the measured solubilities for bulk samples[13] and an extrapolation of Sieverts law. It can be seen that all our measurements are between these two curves. We find strong deviations from the bulk behavior at the higher hydrogen concentrations. Up to a concentration of about 25 at. % no significant thickness dependence was found and there exists no indication of a possible phase transition; the flat region (see bulk behavior in Fig. 4), which is typical for the nearby coexistence region, is especially not seen.

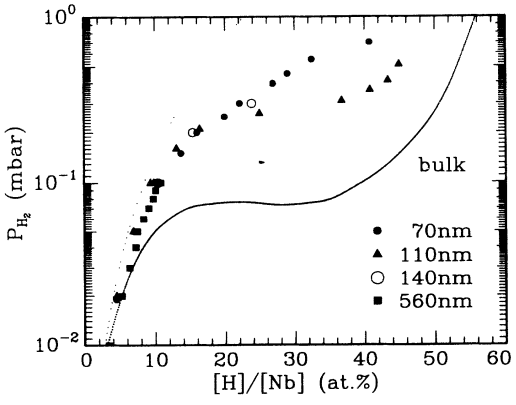

FIG. 4. Hydrogen solubility for various Nb films with different thicknesses at a temperature of 200 °C. The solid line in the solubility for bulk material (Ref. 13) while the dotted line is an extrapolation of Sieverts law which describes the solubility for low H concentrations.

The data shown in Fig. 4 were obtained in the first charging cycle on virgin films in measurements with monotonically increasing hydrogen concentrations. We found that the solubility is reversible for low concentrations but not after heavy charging. We have checked the reversibility in several cases. For the 140-nm thick film we found complete reversibility up to a concentration of 25 at. %. For the 70-nm film after charging to 35 at. % almost complete removal of hydrogen was possible in vacuum, whereas for the 110-nm-thick film, this was not possible anymore after the charging to 40 at. %. In case of the 560-nm-thick film, the reversibility already broke down below 11 at. %. Our experience with films of different thicknesses is that there exists a critical concentration, which decreases with film thickness, up to which the solubility is reversible. Beyond this concentration the films are irreversibly changed and retain a high concentration of hydrogen after removing the external hydrogen atmosphere.

A complete absorption and desorption cycle at a temperature of 187 °C is shown in Fig. 5. It can be seen that, after this heavy charging, no complete desorption is possible and hydrogen remains in the sample at a concentration of about 36 at. % even at 10^{-5} mbar. The film is irreversible distorted.

At low temperatures, which are interesting because of the α-α' phase separation, the absorption and desorption process is very slow. The time constant at 165 °C is approximately $\frac{1}{2}$ h; therefore, the measurements become very time consuming. At low temperatures the equilibrium concentration was extrapolated from the increase of

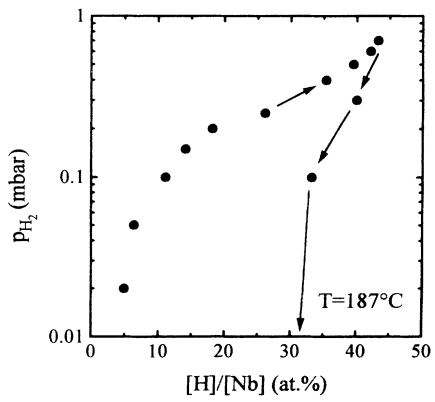

FIG. 5. Charging and decharging of a 100-nm-thick Nb film at a temperature of 187 °C. A fairly high H concentration remains in the film after removing the external H_2 atmosphere.

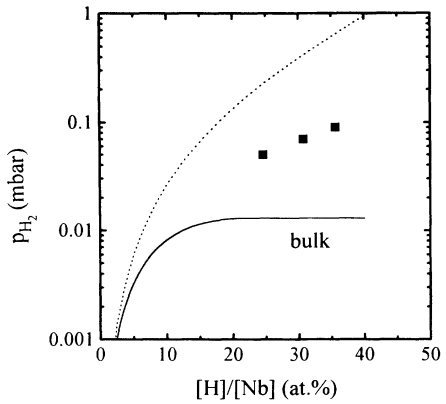

FIG. 6. Hydrogen solubility in a 100-nm-thick Nb film at 166 °C (below the temperature of the α-α' phase transition in bulk). The solid line is the solubility for the bulk (Ref. 13), the dotted line is again an extrapolation of Sieverts law. No sign of a phase transition is seen.

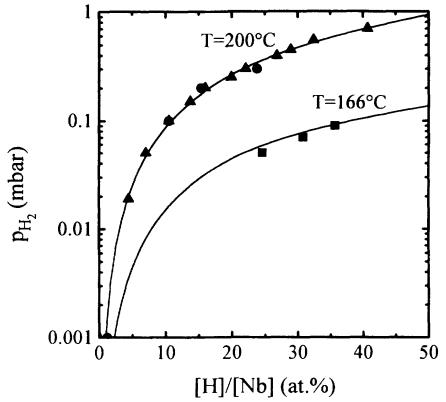

FIG. 7. Hydrogen solubility in Nb films at two different temperatures. The solid lines are fits with Eq. (5) (lattice gas model) using the same parameters in the two cases.

the concentration using a simple model for the absorption process.[6] The resulting solubility is shown in Fig. 6. Again, the predictions of Sieverts law and the known bulk solubility are included. As at 200 °C, no sign of a phase separation (plateau) is observed although the temperature for these measurements was below the critical temperature for the α-α' phase transitions in bulk. The data show that, in agreement with x-ray data,[3] the formation of the α' phase is suppressed in epitaxial films.

V. DISCUSSION

A successful model for the analysis of the Nb-H bulk phase diagram is the so-called lattice gas model where one assumes that hydrogen atoms reside at certain interstitial sites in the lattice (tetrahedral in the case of Nb) and that the occupation is either 0 or 1. The H at the different sites interact with the host lattice and with each other. Using mean-field theory, the solubility of H in the lattice can be calculated.[14]

In thermodynamic equilibrium the chemical potentials of the external and internal regions are equal. This yields to the relation

$$\mu_g = 2\mu_\alpha \,, \tag{2}$$

where μ_g is the chemical potential of the H_2 gas and μ_α that of the dissolved hydrogen in the Nb lattice. The factor 2 arises from the fact that hydrogen exists in molecular form (H_2) in the gas but as atomic hydrogen in the metal. With

$$\mu_g = kT \ln p + \mu_0^g \tag{3}$$

and

$$\mu_\alpha = \mu_0^\alpha - uc + kT \ln \frac{c}{1-c} \,, \tag{4}$$

the solubility for the lattice gas can be calculated to

$$p = \exp\left[\frac{2\mu_0^\alpha - \mu_0^g}{kT}\right] \exp\left[\frac{-2uc}{kT}\right] \left[\frac{c}{1-c}\right]^2 . \tag{5}$$

Here c is the number of occupied sites divided by the total number of available sites (one for each Nb atom), i.e., c is proportional to the H concentration, u is the H-H interaction energy, p is the external H_2 pressure, and μ_0^g, μ_0^α is the standard potential. For small concentrations where the H-H interaction can be neglected, this expression reduces to the well-known Sieverts law which states that the H concentration is proportional to the square root of the H_2 pressure ($c = K\sqrt{p}$). At higher concentrations the interaction can no longer be neglected. The solubility deviates from Sieverts law as found in the experiment.

A fit of the measured film solubility with Eq. (5) is shown in Fig. 7. At both temperatures, the fit using the same parameters for μ_0 and u agrees very well with the measured data over the whole concentration range. We find $2\mu_0^\alpha - \mu_0^g = 0.4$ eV which is the same as in bulk, indicating that the metal-hydrogen interaction is the same in the film as in the bulk. However, the H-H interaction is strongly reduced. We find $u = 0.1$ eV for the film, whereas the corresponding value for the bulk is $u \approx 0.2$ eV.[15] This reduction of the H-H interaction energy is understandable in terms of the elastic theory. It can be shown that the H-H interaction produced by long-ranged strain fields is attractive for samples with free surfaces but that this attractive interaction becomes repulsive when all surfaces are clamped.[15–18] In our case, the Nb layer is clamped to the sapphire substrate due to the epitaxial growth. Therefore, it is plausible that the special boundary condition of epitaxial films reduces the interaction energy as found in the experiment. Quantitative calculations on this effect are not available.

A reduction of the H-H interaction in thin films compared to the bulk had been reported before for hydrogen in thin polycrystalline Pd films on quartz substrates.[20] There, too, the authors attribute the effect to the elastic boundary conditions at the film-substrate interface.

VI. CONCLUSIONS

In this paper, direct measurements of the H solubility in thin Nb layers are reported. Some earlier works on

this subject depend on indirect measures of the H concentration (electric resistivity or volume expansion[2,19]). Using the bulk behavior of these indirect measures to infer hydrogen concentrations can lead to wrong results in films. We find indeed a different behavior. The increased solubility reported in these earlier studies could not be confirmed. We find instead that the solubility in film is the same as in bulk for low concentrations and that it is strongly reduced at higher external H_2 pressures. No indication of the precipitation of the α' phase is observed in agreement with the x-ray studies. The analysis of the data with a mean-field lattice gas model yields that the Nb-H interaction in films is the same as in bulk but the H-H interaction energy is reduced by a factor of 2. This reduction is qualitatively expected in the framework of the elastic theory with special boundary conditions but quantitative predictions do not exist yet.

ACKNOWLEDGMENT

We thank B. Mertesacker for help in the experimental work.

[1]T. Schober and H. Wenzel, in *Hydrogen in Metals II,* edited by G. Alefeld and J. Völkl, Topics in Applied Physics Vol. 29 (Springer-Verlag, Berlin, 1978), p. 11.

[2]P. F. Miceli, H. Zabel, and E. Cunningham, Phys. Rev. Lett. **54**, 917 (1985).

[3]P. F. Miceli, H. Zabel, J. A. Dura, and C. P. Flynn, J. Mater. Res. **6**, 964 (1991).

[4]J. Steiger, S. Blässer, O. Boebel, J. Erxmeyer, B. Mertesacker, and A. Weidinger, Z. Phys. Chem. Neue Folge (to be published).

[5]S. Durbin, J. E. Cunningham, and C. P. Flynn, J. Phys. F **12**, L75 (1982).

[6]M. A. Pick, J. W. Davenport, M. Strongin, and G. J. Dienes, Phys. Rev. Lett. **43**, 286 (1979).

[7]W. A. Lanford, Nucl. Instrum. Methods **149**, 1 (1978).

[8]S. Blässer, J. Steiger, and A. Weidinger, Nucl. Instrum. Methods B (to be published).

[9]C. Sürgers and H. v. Löhneisen, Appl. Phys. A **54**, 350 (1992).

[10]F. J. Lamelas, Hui He, and R. Clarke, Phys. Rev. B **38**, 6334 (1988).

[11]J. P. Biersack, Nucl. Instrum. Methods **182/183**, 199 (1981).

[12]J. P. Biersack, Z. Phys. A **305**, 95 (1982).

[13]J. A. Pryde and C. G. Titcomb, Trans. Faraday Society **65**, 2758 (1969).

[14]G. Alefeld, Phys. Status Solidi **32**, 67 (1969).

[15]G. Alefeld, Ber. Bunsenges. Phys. Chem. **76**, 746 (1972).

[16]J. D. Eshelby, J. Appl. Phys. **25**, 255 (1954).

[17]J. D. Eshelby, Acta Metall. **3**, 487 (1955).

[18]H. Wagner and H. Horner, Adv. Phys. **23**, 587 (1974).

[19]S. Moehlecke, C. F. Majkrzak, and M. Strongin, Phys. Rev. B **31**, 6804 (1985).

[20]R. Feenstra, G. J. de Bruin-Hordijk, H. L. M. Bakker, R. Griessen, and D. G. de Groot, J. Phys. F **13**, L13 (1983).